Indian Journal of Chemistry
Vol. 59B, October 2020, pp. 1564-1574

Pyrene appended terpyridine derivatives as electrochemiluminescence material for OLEDs: Characterization of photo-physical, thermal and electrochemical properties

Gorakala Umasankar[a,c], Manohar Reddy Busireddy[a,b,c], Bhanuprakash Kotamarthi[b,c], Galla V Karunakar[a,c] & Vaidya Jayathirtha Rao*[a,c]

[a] Fluoro and Agrochemicals Department, CSIR-Indian Institute of Chemical Technology, Uppal Road Tarnaka, Hyderabad 500 007, India

[b] Catalysis and Fine Chemicals Department, CSIR-Indian Institute of Chemical Technology, Tarnaka, Hyderabad 500 007, India

[c] Academy of Scientific and Innovative Research (AcSIR), Sector 19, Kamla Nehru Nagar, Ghaziabad, Uttar Pradesh 201 002, India

E-mail: vaidya.opv@gmail.com; bprakash@iict.res.in

Received 26 October 2019; accepted (revised) 14 February 2020

Three new terpyridine appended pyrene derivatives (**Pyr-Tp**, **Pyr-Ph-Tp**, and **Pyr-Bp-Tp**) have been synthesized by condensation and Suzuki-Miyaura reaction. The photo-physical, electro-chemical and thermal properties of these compounds have been investigated in detail. DFT studies have been carried out to understand the structure-property relationships at the molecular level. Synthesized fluorophores displayed high quantum yield (70-96%) of fluorescence due to triplet to singlet intramolecular energy transfer, delayed fluorescence and positive solvatochromism indicating the presence of intra-molecular charge transfer excited state. In addition, they have high thermal decomposition temperature (T_d: 390-450°C), melting temperature (T_m: 180-220°C) and further with suitable oxidation and reduction potentials makes them favourable molecules for OLED fabrications.

Keywords: Terpyridine-pyrene derivatives, fluorescence quantum yield, delayed fluorescence, phosphorescence, thermal stability, oxidation and reduction potentials, OLED materials

After the innovation of Tang and Vanslyke[1], Organic light emitting diodes (OLEDs) have gained a huge interest to understand its complicated mechanism of functioning and also to improve performances for practical applications[2-5]. OLEDs are becoming to be promising candidates for flat panel display and solid state lighting sources[6]. OLEDs are advanced with color purity, low driving voltage, wide viewing angle, eco-friendly, self-emitting, high brightness and simple device structure with cost-effective properties were assisted successfully for their commercial applications[7-10]. Since the numerous efforts have been put with OLEDs to develop a triplet harvesting emitter which overcome their traditional efficiency barrier 5% (1st generation of OLEDs). Although 100% IQE attained in phosphorescence organic light emitting diodes (PHOLEDs), involving rare earth metal (**Pt** and **Ir**) utilization and poor stability[11-15] further declined their practical application.

Currently, harvesting the triplet excitons into radiative transition is an emerged feature for fluorescent OLEDs in order to overcome 5% efficiency barrier[16,17]. Triplet-triplet annihilation (TTA)[18], Thermal activated delayed fluorescence (TADF)[19], and Hybridised local charge transfer state (HLCT)[20] are promising approaches for harvesting triplet excitons in device operation. In addition, the charge balance and transport are essential parameters for monitoring the recombination process exactly at emissive layer of device configuration and improve OLEDs performances[21,22]. Hence, both the parameters of harvesting triplet excitons and charge carriers are collectively increased the demand of multifunctional emitter for cost effective OLED fabrications. Furthermore, emitter with electron transports are less explored relatively to emitter with hole transporter is due to high mobility of holes compare to electron[23]. Therefore to improve electron transport property and

balance the charge, many electron deficient end groups of oxadiazole[24], phosphine oxide[25], triazine[26], benzimidazole[27], terpyridine and quinoxalines[28] are comprehensively selected and further their additional beneficiaries have been proven them as promising candidates for OLEDs applications.

Considering the above factors here we have focused in designing multifunctional emitter from pyrene. The high fluorescence emission, thermal stability and charge carrier properties of pyrene are suitable for designing multifunctional emitter[29,30]. End groups functionalized pyrene as a multi-functional emitter have been explored for OLED applications. Keawin et al. designed dendrimers structure from pyrene and carbazole, which resulted as blue emitters with hole-transporting materials[31]. Another pyrene based multifunctional molecule was synthesized by Mallesham et al, which acts as a blue emitter and electron transporting material[25]. A pyrene-appended dimethyl phenyl derivative was used (Chou et al.) to harvest the triplet states through the reverse intersystem crossing[18].

Terpyridine moiety, due to its electron withdrawing strength can affect the electron affinity in pyrene and expected to enrich charge carrier property in fluorophore[32,33]. We have designed and synthesized three derivatives of pyrene appended terpyridine as shown in Figure 1, where pyrene and terpyridine directly linked **Pyr-Tp**, the phenyl and biphenyl used as a spacer in **Pyr-Ph-Tp** and **Pyr-Bp-Tp** respectively. From the investigation it is seen that the three derivatives displayed high quantum yield, exhibited delayed fluorescence and charge transfer state. Theoretical studies assigned the dihedral angle around 55-57° between pyrene and adjacent aryl group. Further their increasing pattern of thermal stability, appropriate HOMO and LUMO energy levels strongly convince that these synthesized fluorophores have a potential to perform as a capable emitter for OLEDs applications.

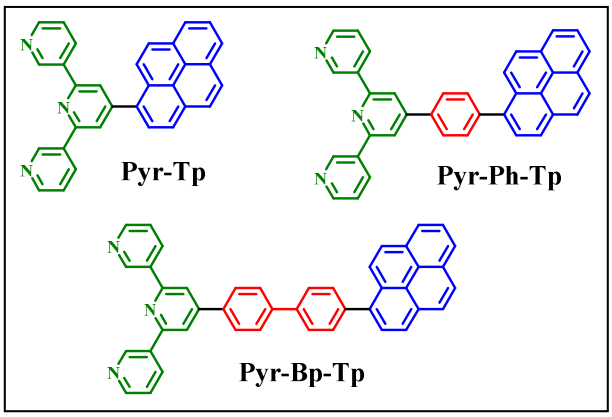

Figure 1 — Chemical structures of the synthesized fluorophores

Experimental Section

Materials and instruments

Unless otherwise specified, all the reactions were carried out under nitrogen atmosphere with standard Schlenk techniques. All the required reagents and solvents were purchased from commercial sources and used without further purification. Solvents used in this work such as tetrahydrofuran (THF) were distilled over sodium/Benzophenone, N, N'-dimethylformamide (DMF) and dichloromethane (CH_2Cl_2) were dried over 3 Å molecular sieves to remove the moisture under nitrogen atmosphere. Synthesized compounds structures were analysed by ^{1}H NMR and ^{13}C NMR spectra on a Bruker Avance (300,400 and 500, MHz) spectrometer in $CDCl_3$ with TMS as the internal standard. Mass spectra and high-resolution mass spectra (HRMS) of target compounds were recorded using electrospray ionization (ESI) ion trap mass spectrometry. The UV-Vis absorption and steady-state fluorescence spectra were measured using Agilent Technologies Cary Series UV-Vis-NIR spectrometer and Agilent Technologies Cary Eclipse spectro-fluorometer, respectively. The fluorescence quantum yields (Φ_f) were determined by integrating the fluorescence bands and by using 9, 10-diphenylanthracene (DPA) as standard. Delayed fluorescence (DF), phosphorescence, and phosphorescence lifetime measurements were carried out by using Fluorolog instruments at room temperature (RT) and 77K. TGA and DSC experiments were conducted under inert atmosphere on Exstar TG/TGA 7200 and Exstar DSC 7020 instruments, respectively with 10°C/min heating and cooling rate. Cyclic voltammetry (CV) measurements were recorded by PC-controlled CHI 62C electrochemical analyser in dry CH_2Cl_2 solvent at a scan rate of 100 mV s^{-1} using tetrabutylammonium perchlorate (0.1 M) as the supporting electrolyte. The glassy carbon, standard calomel electrode (SCE) and platinum wire were used as working, reference and counter electrode, respectively.

Computational details

All theoretical calculations have been carried out in this study using Gaussian 09 software package within the framework of density functional methods[34]. Ground state geometry of the molecules were

optimized in gas and solution phase at the density functional theory (DFT)/B3LYP/6-311G(d,p) level of theory with no symmetry constraints imposed[35]. Optimized geometries were subjected to vibrational analysis to ensure that they were no imaginary frequency and hence global minima on the potential energy surface. The optimized (stable) geometries were taken as the starting point for time-dependent density functional theory (TD-DFT) calculations. The iso-density surface plots of frontier molecular orbitals were generated from the population analysis calculations on optimized geometries using Gauss View package[36]. Singlet excited states were calculated using TD-DFT methods. To simulate the experimental absorption spectra of the compounds, calculates PBE0 has been used with a basis set of 6-311G (d,p)[37,38] and carried out in chloroform to include solvent effects is the integral equation formalism variant of the polarisable continuum model (IEFPCM) implemented in the Gaussian package[39].

Synthetic procedure

Synthesis of 4'-phenyl-3, 2':6', 3''-terpyridine (Ph-Tp)

To the solution of benzaldehyde (2 g, 18 mmol), 3-acetyl pyridine (4.1 g, 36 mmol in 150 mL round-bottom flask, then added 50 ml of ethanol and stirred until clear solution appeared. KOH (1.05 g, 18 mmol) dissolved in 80 mL of liquor NH_3 was added slowly to the reaction mixture (additionally adding ammonium solution in between to the reaction mixture for avoiding ammonium deficiency). The resulting reaction mixture was stirred at room temperature for 4 h (reaction progress was thoroughly monitored by TLC), during which a precipitate was formed. The precipitate was filtered through a Buchner funnel, washed with water and ethanol resulting in a light yellow coloured compound which was then purified by silica gel column chromatography (20% ethyl acetate in hexane as an eluent) to yield the title compound as light yellow coloured solid (50% of 2.2g).

^{1}H NMR (400 MHz, $CDCl_3$, δ ppm): 9.39 (d, *J* = 1.5 Hz, 2H), 8.72 (dd, *J* = 4.8 Hz, 2H), 8.53 (tt, *J* = 3.9 Hz, 2H), 7.96 (s, 2H), 7.77 (dd, *J* = 8.4 Hz, 2H), 7.59-7.50 (m, 3H), 7.48 (dd, *J* = 8.3 Hz, 2H); ^{13}C NMR (100 MHz, $CDCl_3$, δ ppm): 155.3, 150.9, 150.2, 148.4, 138.2, 134.6, 134.5, 129.4, 129.3, 127.1, 123.6, 117.7; ESI-MS (m/z): 310 [M+1], ESI-HRMS [M+H] (m/z):calc. for $C_{21}H_{16}N_3$is 310.3718; found 310.1370; m.p.140-142°C.

Synthesis of 4'-(pyren-1-yl)-3,2':6',3''-terpyridine (Pyr-Tp)

This compound was synthesized according to the procedure given above for **Ph-Tp**, but by using pyrene aldehyde (2 g, 8 mmol), 3-acetyl pyridine (1.9 g, 17mmol) as synthetic precursor to obtain the desired product as light yellow color solid. Yield 50%(~2g).

^{1}H NMR (400 MHz, $CDCl_3$, δ ppm): 9.44 (d, *J* = 1.9 Hz, 2H), 8.72 (d, *J* = 4.76 Hz, 2H), 8.56 (d, *J* = 7.82 Hz, 2H), 8.31-8.05 (m, 11H), 7.48 (dd, *J* = 7.9 Hz, 2H);^{13}C NMR (100 MHz, $CDCl_3$, δ ppm): 154.9, 151.5, 150.2, 148.5, 134.5, 134.1, 131.6, 131.3, 130.7, 128.6, 128.2, 127.2, 126.8, 126.3, 125.7, 125.4, 124.9, 124.8, 124.6, 123.9, 123.6, 121; ESI-MS (m/z): 434 [M+1], ESI-HRMS [M+H] (m/z):calc. for $C_{31}H_{20}N_3$ is 434.5106; found 434.1680;m.p. 220-222°C.

Synthesisof 4'-(4-(pyren-1-yl) phenyl)-3, 2':6', 3''-terpyridine (Pyr-Ph-Tp)

Pyr-Ph-Tp was synthesized by Pd-catalysed Suzuki-Miyaura cross coupling reaction. 4'-(4-bromophenyl)-3,2':6',3"-terpyridine (1 g, 2 mmol), pyrene borate (1.09 g, 3 mmol), and sodium carbonate (2.18 g, 20 mmol) were mixed in dry THF (50 ml), ethanol and water (1:2 ratio) were added to the reaction mixture and purge nitrogen for 15 min. Pd $(PPh_3)_4$ catalysts was added to reaction mixture and refluxed for 12 h under N_2 atmosphere. After completion of reaction, reaction mixture was cooled to room temperature and filtered through the celite pad to remove the inorganic impurities and extracted with ethyl acetate. The organic layer was thoroughly washed with water and then dried over anhydrous Na_2SO_4. After the evaporation of solvent, the crude product was purified by column chromatography over silica gel using a mixture of ethyl acetate and petroleum ether (1:2) as eluent to afford the desired product as a yellow coloured solid. Yield 50% (0.75 g).

^{1}H NMR (400 MHz, $CDCl_3$, δ ppm):9.45 (d, *J* = 1.3 Hz, 2H), 8.73 (d, *J* = 3.7 Hz, 2H), 8.59 (tt, *J* = 1.9 Hz, 2H), 8.29 (d, *J* = 7.8 Hz, 1H), 8.25 (d, *J* = 2.6 Hz, 1H), 8.23 (s, 1H), 8.22 (d, *J* = 7.4 Hz, 1H), 8.14 (s, 2H), 8.11 (d, *J* = 5.5 Hz, 3H), 8.07-8.03(m, 2H), 7.99 (d, *J* = 8.3 Hz, 2H), 7.86 (d, *J* = 8.3 Hz, 2H), 7.52 (dd, *J* = 8.06 Hz, 2H); ^{13}C NMR (100 MHz, $CDCl_3$, δ ppm): 155.5, 150.5, 150.2, 148.4, 146.7, 142.6, 137.0, 134.7, 134.6, 132.2, 131.5, 131.4, 130.9, 127.8, 127.8, 127.7, 127.4, 127.3, 127.2, 126.1, 125.3, 125.0, 124.8, 124.7, 123.6, 117.7; ESI-MS (m/z): 510

[M+1], ESI-HRMS [M+H] (m/z): calc. for $C_{37}H_{24}N_3$ is 510.6066; found 510.1980; m.p. 230-232°C.

Synthesis of4'-(4'-(pyren-1-yl)-[1,1'-biphenyl]-4-yl)-3,2':6',3''-terpyridine(Pyr-Bp-Tp)

This compound was synthesized according to the synthetic procedure of **Pyr-Ph-Tp** given above but by using 4'-(4'-bromo-[1,1'-biphenyl]-4-yl)-3,2':6',3''-terpyridine (1 g, 2 mmol) and pyrene borate (0.915 g, 2.8 mmol) and sodium carbonate (1.83 g, 17 mmol) as synthetic precursor (yield 50%, 0.80 g).

^{1}H NMR (400 MHz, $CDCl_3$, δ ppm): 9.43 (d, *J* = 1.43 Hz, 2H), 8.74 (d, *J* = 4.5 Hz, 2H), 8.58 (tt, *J* = 7.94 Hz, 2H), 8.29 (d, *J* = 3.0 Hz, 1H), 8.26 (d, *J* = 1.46 Hz, 1H), 8.24 (d, *J* = 7.7 Hz, 1H), 8.21 (d, *J* = 7.21 Hz, 1H), 8.13 (s, 2H), 8.09 (d, *J* = 9.6 Hz, 4H), 8.04 (d, *J* = 1.95 Hz, 1H), 7.94 (d, *J* = 2.2 Hz, 4H), 7.90 (d, *J* = 8.1 Hz, 2H), 7.80 (d, *J* = 8.19 Hz, 2H), 7.52 (dd, *J* = 7.70 Hz, 2H); ^{13}C NMR (100 MHz, $CDCl_3$, δ ppm): 155.4, 150.3, 150.2, 148.3, 141.9, 140.8, 138.8, 137.0, 136.9, 134.6, 134.5, 131.4, 131.2, 130.9, 130.6, 128.4, 127.9, 127.7, 127.6, 127.5, 127.3, 127.0, 126.0, 125.2, 125.1, 124.9, 124.8, 124.7, 123.6, 117.5; ESI-MS (m/z): 586 [M+1], ESI-HRMS [M+H] (m/z): calc. for 585.6946; found 586.2298; m.p. 240-242°C.

Results and Discussion

Synthesis and characterization

All target compounds (**Pyr-Tp**, **Pyr-Ph-Tp**, and **Pyr-Bp-Tp**) shown in Figure 1, were prepared according to a multiple synthetic pathway as illustrated in Scheme I, intermediate synthetic route as depicted in Scheme S1 (ESI) and their detailed synthetic procedures provided in the Experimental Section. Pyrene was brominated to obtain bromopyrene (**1**), bromopyrene was treated with n-butyl lithium at −78°C and then added 2-isopropoxy-4,4,5,5-tetramethyl-1,3,2-dioxaborolane to obtain the boronate intermediate (**2**)[25]. Pyrene-1-carbaldehyde (**3**) was prepared from pyrene formylation, by subjecting it to 1,2-dichloro dimethyl ether/$TiCl_4$ [40]. 4,4'-Dibromo-1,1'-biphenyl treated with n-butyl lithium at −78°C followed by the addition of DMF to obtained 4'-bromo-[1,1'-biphenyl]-4-carbaldehyde (**4**) [41]. Intermediates **5**, **6**, **Ph-Tp** and **Pyr-Tp** were synthesized using acetyl pyridine and corresponding

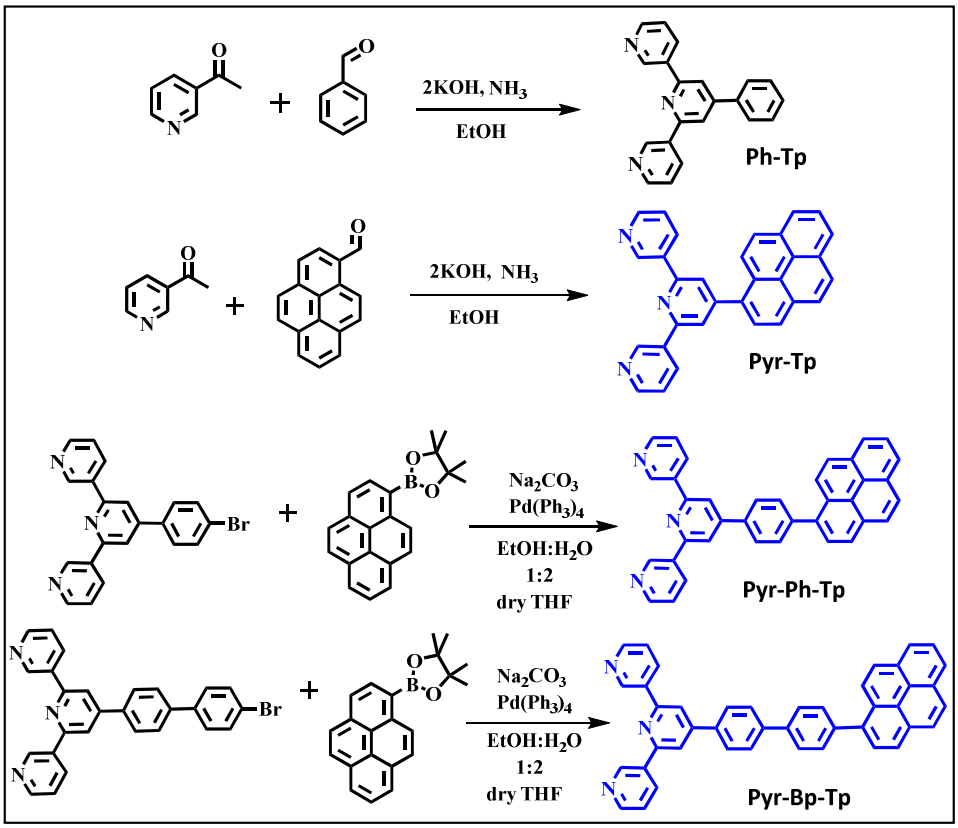

Scheme I — Synthetic route for desired fluorophores

aldehydes (benzaldehyde, 4-bromo-benzaldehyde and **3**, respectively)[32]. This reaction involves Claisen condensation, Micheal addition, and Hantz pyridine reaction sequentially. **Pyr-Ph-Tp** and **Pyr-Bp-Tp** were synthesized by treating the corresponding terpyridine bromo derivatives (**5** and **6** respectively) with 4,4,5,5-tetramethyl-2-(pyren-1-yl)-1,3,2-dioxaborolane (**2**) in Suzuki cross coupling path way. Desired fluorophores were obtained in the range of 50-55% yield. All the synthesized molecules were thoroughly characterized using ^{1}H NMR (Figures S8-S11, ESI), ^{13}C NMR (Figures S11-S15, ESI), LCMS (Figures S16-S19, ESI) and HRMS (Figures S20-S23, ESI) analysis.

Molecular geometry and orbitals of the fluorophores

The optimized structures of **Pyr-Tp**, **Pyr-Ph-Tp**, and **Pyr-Bp-Tp** are almost non-planar. The dihedral angle between pyrene and adjacent aryl group's fall in the range of 55-57° are shown in Figure 2. The negligible deviation of dihedral angle in derivatives indicates pyrene position regarding entire molecule is not much affected with substitution of phenyl and biphenyl spacer.

Frontier molecular orbital diagrams are shown in Figure 3. In **Pyr-Tp**, the HOMO is dispersed mostly on pyrene and phenyl rings and negligible dispersed on pyridine ring of terpyridine part. Whereas in **Pyr-Ph-Tp** and **Pyr-Bp-Tp**. HOMO is completely confined on pyrene and phenyl part. The LUMO is in all three derivatives is dispersed on pyrene, phenyl and pyridine ring of terpyridine part[42]. All of these molecules displayed HOMO to LUMO transition.

Photo physical properties

The UV-Vis absorption spectra of three derivatives were recorded in solution ($1x10^{-5}$ M) and in the thin film state to check suitability of compounds for electro luminescence applications. The corresponding spectra are presented in Figure 4a and (Figure S2a (ESI), their relevant data are compiled in Table I.

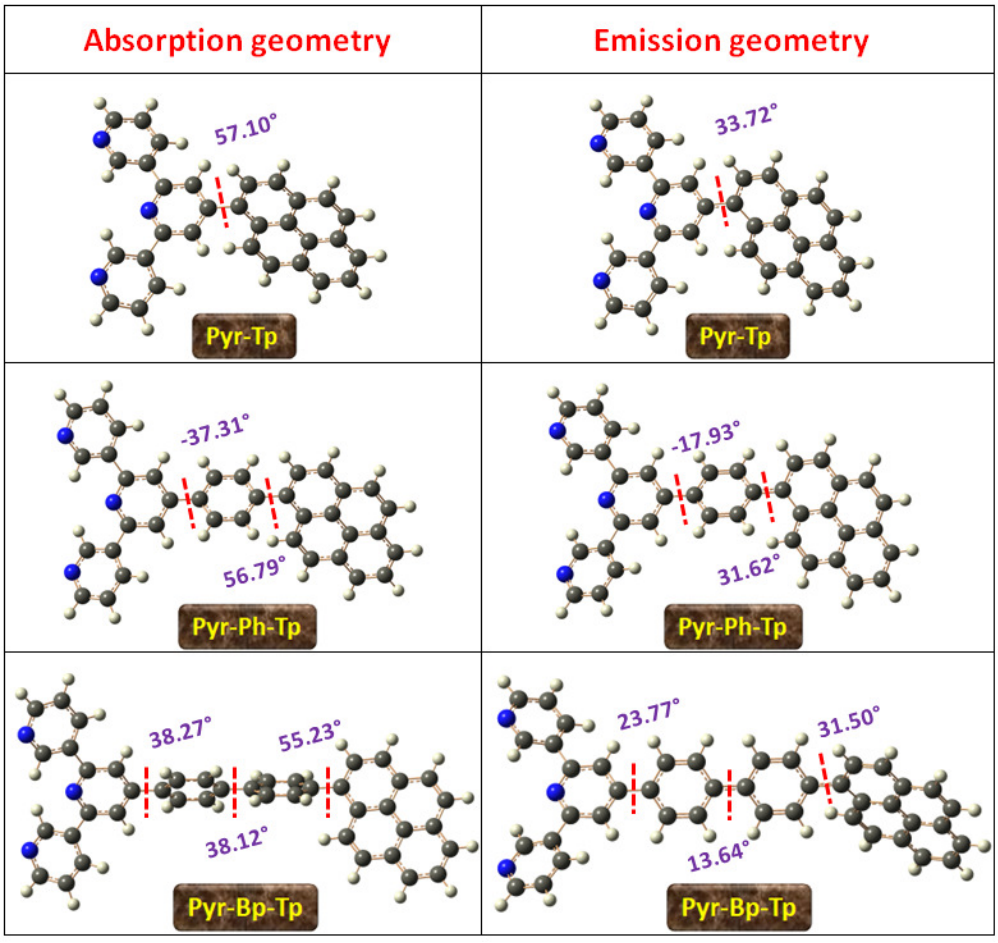

Figure 2 — Optimized configuration of fluorophores

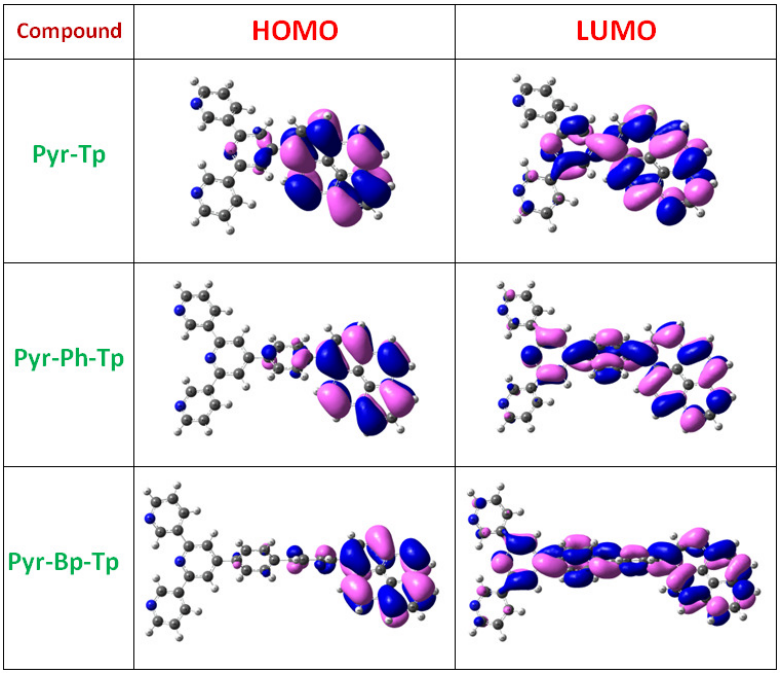

Figure 3 — FMOs orbital diagrams of fluorophores

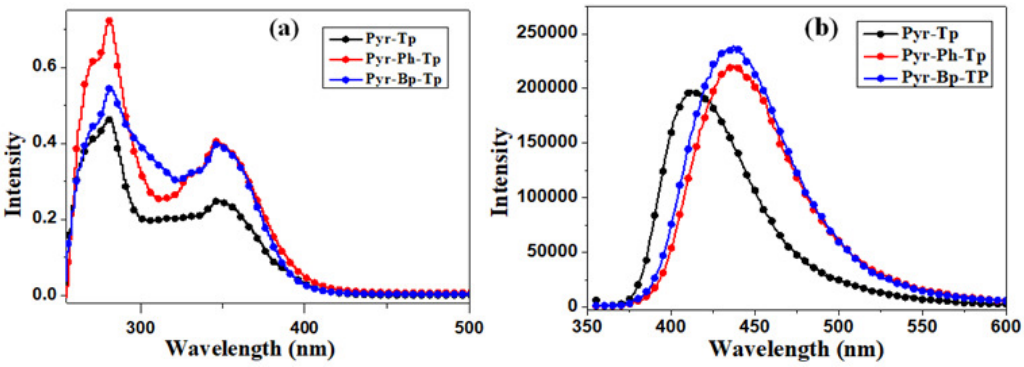

Figure 4 — (**a**) Absorption spectra in solution, (**b**) Emission spectra in solution

Table I — UV-Vis absorption, fluorescence data of **Pyr-Tp**, **Pyr-Ph-Tp** and **Pyr-Bp-Tp**

Materials	λ_{abs} (nm)[a] sol	λ_{abs} (nm)[b] film	λ_{em} (nm)[a] sol	λ_{em} (nm)[b] film	Φ_f[c]
Pyr-Tp	349	358	413	476	0.69
Pyr-Ph-Tp	347	366	432	470	0.85
Pyr-Bp-Tp	347	359	435	460	0.95

[a]Recorded in chloroform at 10^{-5}M.
[b]Recorded in thin film state.
[c]Fluorescence quantum yield measured in cyclo hexane, relative to 9,10-diphenyl anthracene (Φ_f = 0.9 in cyclohexane).

The absorption spectra in chloroform solution exhibit two distinctive absorption bands (i.e. 270 nm and 350 nm), respective shorter wavelength (270 nm) is ascribed to a localized aromatic π-π* transition of the conjugated backbone, while the bands at longer wavelength (350 nm) is mainly attributed to an intra-molecular charge transfer (ICT) transition from the pyrene to terpyridine[33,40-42,43], because of loss of fine structure in pyrene absorption. Similar pattern of absorption spectra with negligible shift were appeared in various solvents of different polarities (hexane, acetonitrile, DMF and methanol), ensure that there is

no change in dipole moment of derivatives geometry during the excitation. The thin film state, the absorption spectra observed with small red shift (9-16 nm) and informs that there is less or negligible intermolecular interactions or change in dihedral angle in the solid state. TD-DFT simulated, UV-Vis absorption spectra obtained for **Pyr-Tp**, **Pyr-Ph-Tp** and **Pyr-Bp-Tp** in solvent phase using PBE0/6-311G(d,p) are displayed in Figure S1 (ESI). The absorption spectra was obtained by convoluting Gaussian functions with FWHM as 3000 cm^{-1} using Gausssum package. PBE0 framework shows reasonable agreement with the experimental absorption data and the trend is consistent with experimental observation (Table II). The computed energies of vertical excitations along with oscillator strength and compositions in terms of molecular orbitals are summarized in Table S1 (ESI). The oscillator strength of these compounds gradually increased with increasing number of phenyl spacers in the molecular backbone. The calculated emission energies using TD-DFT are included in Table II. The emission energies (TD-DFT) are 438nm, 473nm and 485nm respectively for **Pyr-Tp**, **Pyr-Ph-Tp** and **Pyr-Bp-Tp**, are in slightly overestimated with the experimental emissions.

Fluorescence emission in solution state falls in the range of 412-435 nm and 460-476 nm for thin film state, indicating that promising blue emitter for OLEDs applications. The quantum yield of derivatives were calculated by taking diphenylanthracene (DPA) as internal standard and obtained values in the range of 69-96% indicates maximum utilization of singlet excitons/excited state into luminescence[44]. In order to analyze the nature of emission state, the fluorescence was recorded from low concentration ($1x10^{-5}$ M) to high concentration ($1x10^{-2}$ M), where the characteristic pyrene excimer peak was not appeared at high concentration is due to additional terpyridine might maintain non planar geometry even at excited level state, related spectral data are shown in Figure 5. Further fluorescence recorded in various solvents of different polarities, a red shift of 38-70 nm appeared from non-polar hexane to polar acetonitrile/methanol, the spectral data compiled in Table III. The red shift in polar solvents assigned for formation of intramolecular charge transfer (ICT) state of emission[45,46] which is a favourable parameter for reducing the energy gap between singlet and triplet state and makes it feasible for reverse inter system crossing[25,47] and also helps in triplet to singlet intra-molecular energy transfer process[48,49] when singlet state with suitable energy level available within the molecule.

Experimentally the triplet emission was not appeared in synthesized fluorophores, hence the mode of triplet-triplet annihilation (TTA) for delayed fluorescence is ruled out. To understand the exhibited delayed fluorescence in synthesized pyrene derivatives, the phosphorescence spectra of phenyl terpyridine was recorded in ethanol:methanol (1×10^{-5} M) at K the obtained phosphorescence emission (~2.90eV) is closely overlapping to the thin film fluorescence of synthesized derivatives, this closely lying energy levels make it feasible for intersystem crossing from triplet exciton of terpyridine to singlet of synthesized pyrene derivatives[25]. Their characteristic delayed fluorescence lifetimes were also calculated at low temperature (7.0, 7.7 and 8.6 μs for Pyr-Tp, **Pyr-Ph-Tp**, and **Pyr-Bp-Tp** respectively). Above investigation for synthesized fluorophores related to high quantum yield, formation of charge transfer state and delayed fluorescence were emerged features for emitter to perform better in OLED applications. Particularly the overlap of phosphorescence of **Ph-Tp** with thin film state fluorescence indicates energetically favourable condition and also charge transfer nature of the excited state of three pyrene derivatives (Figure 6a and Figure 6b) informs the

Table II — Comparison of the experimental optical properties with the theoretical data

Materials	λ^{sol}_{expt} (nm)[a]	λ^{sol}_{PBE0} nm (f)[b]	λ^{sol}_{expt} Emi (nm)[c]	λ^{sol}_{PBE0} Emi (f)[d]	Major contribution (%)	μ_g (D)[e]	μ_e (D)[f]	μ_{em} (D)[g]
Pyr-Tp	349	360 (0.59)	413	438 (0.97)	H→L (92%)	6.65	8.14	9.00
Pyr-Ph-Tp	347	366 (0.75)	432	473 (1.38)	H→L (96%)	6.57	7.92	8.92
Pyr-Bp-Tp	347	367 (1.00)	435	485 (1.79)	H→L (93%)	6.63	7.93	8.76

[a]Experimental absorption spectra of fluorophores recorded in chloroform (1 x 10^{-5} M solution).
[b]values obtained from TD-DFT/PBE0/6-311G (d, p)/CPCM level of theory (oscillation strength) in chloroform solution.
[c] Experimental emission spectra of fluorophores recorded in chloroform (1 x 10^{-5} M solution).
[d]values obtained from TD-DFT emission /PBE0/6-311G (d, p)/CPCM level of theory (oscillation strength) in chloroform solution.
[e]groundstate,[f]exited state, [g]exited state optimisation dipole moment values obtained from DFT/PBE0/6-311G (d, p).

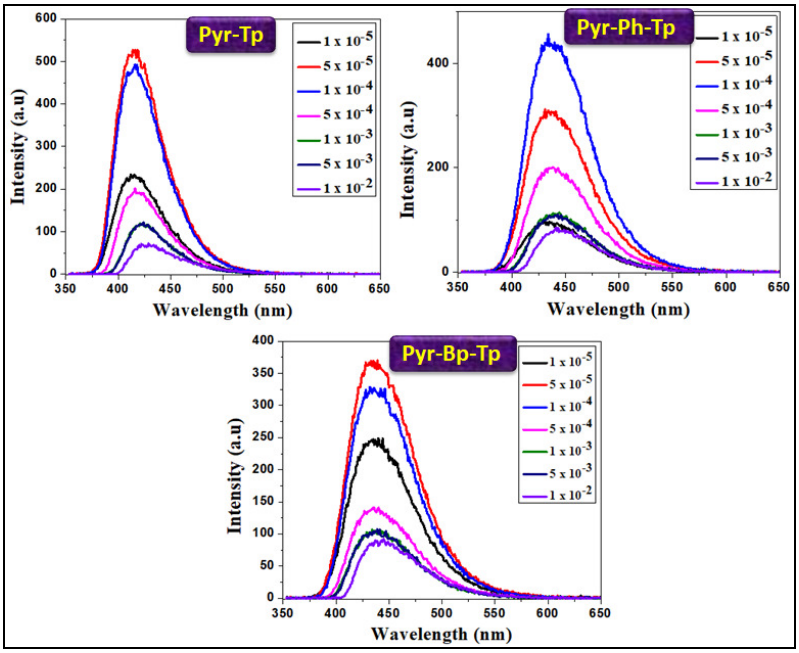

Figure 5 — Fluorescencein chloroform at different concentrations

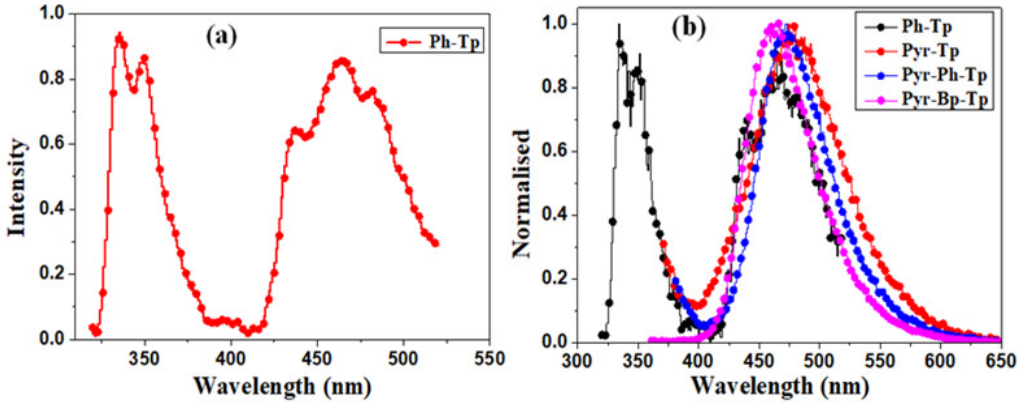

Figure 6 — (**a**) Phosphorescence at 77k, (**b**) Overlay spectra of phosphorescence and thin film fluorescence of fluorophores

Table III — Fluorescence data in different solvents

Materials	Hexane (nm)	$CHCl_3$ (nm)	CH_3CN (nm)	DMF (nm)	MeOH (nm)
Pyr-Tp	404	413	424	425	442
Pyr-Ph-Tp	415	432	456	454	476
Pyr-Bp-Tp	409	435	464	461	479

possibility of triplet to singlet energy transfer[50,51]. Further it is found from the literature that biphenyl triplet energy[52] lies around ~2.99 eV and this is also a favourable arrangement for triplet to singlet energy transfer.

Electrochemical studies

The cyclic voltammograms are displayed in Figure 7 and the corresponding data are summarized in Table IV. All the compounds show oxidation potential in the range of 0.6 – 0.7 V. HOMO of all the compounds are calculated from the empirical formula: $E_{HOMO} = -e[4.4+ E_{OX}]$ eV based on SCE energy level relative to vacuum. The first oxidation peak potential was used to calculate the HOMO and the obtained values are -5.03, -5.05 and -5.08eV for **Pyr-Tp**, **Pyr-Ph-Tp**, and **Pyr-Bp-Tp** respectively. LUMO is estimated from the measured HOMO values and

optical band gap. The values are calculated to be -3.09, -3.03 and -3.03 eV for **Pyr-Tp**, **Pyr-Ph-Tp**, and **Pyr-Bp-Tp** respectively. Upon LUMO energy levels obtained from onset process. The calculated optical band gap ΔE from the intersecting point of absorption and fluorescence spectra, from that obtained ΔE values subtracted from HOMO values.

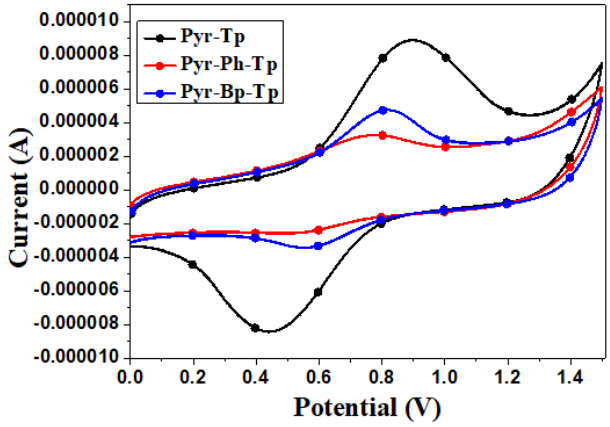

Figure 7 — Cyclic voltagramms of synthesized fluorophores

These appeared impressive electrochemical properties ensure the charge carriers properties in device operation[53,54].

Thermal studies

All the compounds exhibited excellent thermal stability with insignificant weight loss upon 5% decomposition and values are in the range of 410 to 460°C as depicted in Figure 8 and Table V. The decomposition temperature (T_d), increased as the no of phenyl spacers increases between terpyridine and pyrene. These add to the device stability. Glass transition temperature (T_g) did not appear due to the amorphous nature of the compounds[55]. All compounds displayed endothermic peaks corresponding to their melting temperatures (T_m), these values were found to be in the range of 210 to 300°C. The observation is that by increasing number of phenyl spacers increases the melting temperature. The obtained values indicates these are suitable candidates for thermal evaporation process for OLED fabrications[56].

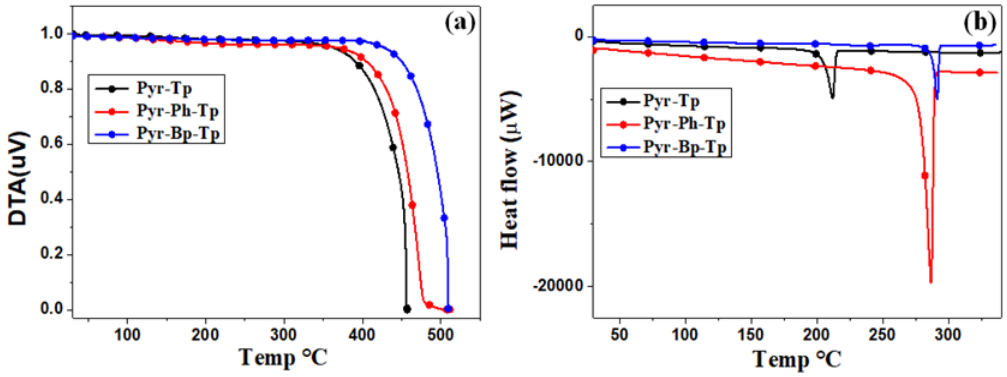

Figure 8 — (**a**) TGA and (**b**) DSC thermo grams of synthesized fluorophores

Table IV — Electrochemical data of the materials

Materials	E_g^{opt} (eV)[a]	E_{OX} (V)	E_{HOMO} (eV)[b]	E_{LUMO} (eV)[c]
Pyr-Tp	3.09	0.63	-5.03	-1.94
Pyr-Ph-Tp	3.03	0.65	-5.05	-2.02
Pyr-Bp-Tp	3.03	0.68	-5.08	-2.05

[a]Estimated from E_g^{opt} = 1240/λ_{onset}, λ_{onset} is onset absorption wavelength in Solution.

[b] HOMO calculated from the formulas E_{HOMO} = -e[4.4 + E_{OX}]

[c]$E_{LUMO} = E_{HOMO} - E_g^{opt}$

Table V — Thermal data of the materials

Materials	Decomposition Temperature (T_d)°C	Melting Temperature (T_m)°C
Pyr-Tp	375	211
Pyr-Ph-Tp	393	286
Pyr-Bp-Tp	441	291

Conclusions

In summary, we have synthesized new series of terpyridine functionalized pyrene compounds (**Pyr-Tp**, **Pyr-Ph-Tp**, and **Pyr-Bp-Tp**) by following Claissen condensation and Pd (0)-catalyzed Suzuki-Miyaura coupling reactions. Their photo physical, electrochemical, and thermal properties were thoroughly investigated. Using DFT methods their functional properties and structural relationship were established. The synthesized fluorophores exhibited good fluorescence quantum yields, delayed fluorescence at RT and 77k, and an efficient charge transfer state. The close spectral overlap of phosphorescence of terpyridine to the fluorescence of desired compounds along with ICT excited state involvement indicates that triplet to singlet energy transfer is very much feasible and this may be responsible for delayed fluorescence with higher quantum yields observed. This can lead to maximised harvesting of the singlet excited states for higher luminescence. The appropriate HOMO/LUMO energy levels favour for efficient charge injection and the obtained thermal property (T_d: 375–441°C and T_m: 211-291°C) indicates a stable emitter for operation at high voltage. We believe that these pyrene-terpyridine derivatives are effective and promising candidates for OLED applications.

Supplementary Information

Supplementary information is available in the website http://nopr.niscair.res.in/handle/123456789/60.

Conflicts of interest

The authors declare no competing financial interest.

Acknowledgements

The authors are thankful to the Director, CSIR-IICT for his constant encouragement of this work (IICT/pubs.2019/373). VJR thanks CSIR-New Delhi for Emeritus Scientist Honour. Funding for this work was supported through a grant [21(1026)/16/EMR-II]. GU and BMR thank UGC-SRF, and also thank AcSIR. IICT/pubs.2019/373.

References

1 Tang C W & Van Slyke S A, *Appl Phys Lett*, 51 (1987) 913.
2 Baldo M A, Lamansky S, Thompson P E & Forrest S R, *Appl Phys Lett*, 75 (1999) 75 4.
3 (a) Burroughs J H, Bradley D D, Broun A R, Marks R N, Mackay K, Friend R H, Burn P L & Holmes A B, *Nature*, 347 (1990) 539; (b) Kido J, Kumara M and Nagai K, *Science*, 267 (1995) 1332; (c) Baldo M A, Thompson M E & Forrest S R, *Nature*, 403 (2000) 750.
4 Baldo M A, Brien D F, You Y, Shoustikov A, Sibley S, Thompson M E & Forrest S R, *Nature*, 395 (1998) 151.
5 Adachi C, Baldo M A, Thompson M E & Forrest S R, *J Appl Phys*, 90(2001) 5048.
6 Baldo M A, Thompson M E & Forrest S R, *Nature*, 403 (2000) 750.
7 Zhou G, Wong W Y, Yao B, Xie Z & Wang L, *Angew Chem Int Ed*, 46 (2007)1149.
8 Lee J, Chen H F, Batagoda T, Coburn C, Djurovich P I, Thompson M E & Forrest S R, *Nature Materials* , 15 (2016) 92.
9 Tagare J & Vaidyanathan S, *J Mater Chem*, *C*, 6 (2018) 10138.
10 Lee J H, Chen C H, Lee P H, Lin H Y, Leung M K, Chiu T L & Lin C F, *J Mater Chem C*, 7 (2019) 5874.
11 Saxena K, Jain V K & Mehta D S, *Optical Materials*, 32 (2009) 221.
12 Lin C H, Chang Y Y, Hung J Y, Lin C Y, Chi Y, Chung M W, Lin C L, Chou P T, Lee G H, Chang C H & Lin W C, *Angew Chem Int Ed*, 50 (2011) 3182.
13 Minaev B, Baryshnikov G & Agren H, *Phys Chem Chem Phys*, 16 (2014) 1719.
14 dos Santos P L, Ward J S, Bryce M R & Monkman A P, *J Phys Chem Lett*, 7 (2016) 3341.
15 Tao Y, Yuan K, Chen T, Xu P, Li H, Chen R, Zheng C, Zhang L & Huang W, *Adv Mater*, 26 (2014) 7931.
16 Luo Y J, Lu Z Y & Huang Y, *Chin Chem Lett*, 27 (2016) 1223.
17 Yang J, Guo Q, Wang J, Ren Z, Chen J, Peng Q, Ma D & Li Z, *Adv Optical Mater*, 6 (2018) 1800342.
18 Chou P Y, Chou H H, Chen Y H, Su T H, Liao C Y, Lin H W, Lin W C, Yen H Y, Chen I C & Cheng C H, *Chem Commun*, 50 (2014) 6869.
19 Zhang L & Cheah K W, *Scientific Reports*, 8 (2018)8832.
20 Chen L, Zhang S, Li H, Chen R, Jin L, Yuan K, Li H, Lu P, Yang B & Huang W, *J Phys Chem Lett*, 9 (2018) 5240.
21 Tong Q X, Lai S L, Chan M Y, Zhou Y C, Kwong H L, Lee C S & Lee S T, *Chem Mater*, 20 (2008) 6310.
22 Hung W Y, Tsai T C, Ku S Y, Chi L C & Wong K T, *Phys Chem Chem Phys*, 10 (2008) 5822.
23 (a) Wang C, Jung G Y, Hua Y, Pearson C, Bryce M R, Petty M C, Batsanov A S, Goeta A E & Howard J A, *Chem Mater*, 13 (2001) 1167; (b) Kulkarni A P, Tonzola C J, Babel A & Jenekhe S A, *Chem Mater*, 16 (2004) 4556.
24 Gong S, Chen Y, Zhang X, Cai P, Zhong C, Ma D, Qin J & Yang C, *J Mater Chem*, 21 (2011) 11197.
25 Mallesham G, Swetha C, Niveditha S, Mohanty M E, Babu N J, Kumar A, Bhanuprakash K & Jayathirtha Rao V, *J Mater Chem*, *C*, 3 (2015) 1208.
26 Chen H F, Yang S J, Tsai Z H, Hung W Y, Wang T C & Wong K T, *J Mater Chem*, 19 (2009) 8112.
27 White W, Hudson Z M, Feng X, Han S & Lu Z H, Wang S, *Dalton Trans*, 39 (2010) 892.
28 Chen C T, Wei Y, Lin J S, Moturu M V, Chao W S, Tao Y T & Chien C H, *J Am Chem Soc*, 128 (2006) 10992.
29 Thomas K J, Kapoor N, Bolisetty M P, Jou J H, Chen Y L, Jou Y C, *J Org Chem*, 77 (2012) 3921.
30 Zhan Y, Peng J, Ye K, Xue P & Lu R, *Org Biomol Chem*, 11 (2013) 6814.
31 Keawin T, Prachumrak N, Namuangruk S, Pansay S, Kungwan N, Maensiri S, Jungsuttiwong S, Sudyoadsuk T & Promarak V, *RSC Adv*, 5 (2015) 73481.

32 Liu C L, Zheng C J, Liu X K, Chen Z, Yang J P, Li F, Ou X M & Zhang X H, *J Mater Chem.C*, 3 (2015) 1068.

33 Schlutter F, Wild A, Winter A, Hager M D, Baumgaertel A, Friebe C & Schubert U S, *Macromolecules*, 43 (2010) 2759.

34 Gaussian 09, Revision B.01, Frisch M J, Trucks G W, Schlegel H B, Scuseria G E, Robb M A, Cheeseman J R, Scalmani G, Barone V, Mennucci B, Petersson G A, Nakatsuji H, Caricato M, Li X, Hratchian H P, Izmaylov A F, Bloino J, Zheng G, Sonnenberg J L, Hada M, Ehara M, Toyota K, Fukuda R, Hasegawa J, Ishida M, Nakajima T, Honda Y, Kitao O, Nakai H, Vreven T, Montgomery J A Jr, Peralta J E, Ogliaro F, Bearpark M, Heyd J J, Brothers E, Kudin K N, Staroverov V N, Kobayashi R, Normand J, Raghavachari K, Rendell A, Burant J C, Iyengar S S, Tomasi J, Cossi M, Rega N, Millam M J, Klene M, Knox J E, Cross J B, Bakken V, Adamo C, Jaramillo J, Gomperts R, Stratmann R E, Yazyev O, Austin A J, Cammi R, Pomelli C, Ochterski J W, Martin R L, Morokuma K, Zakrzewski V G, Voth G A, Salvador P, Dannenberg J J, Dapprich S, Daniels A D, Farkas Ö, Foresman J B, Ortiz J V, Cioslowski J, Fox D J, Gaussian, Inc, Wallingford CT (2009).

35 Bryantsev V S, Diallo M S, Van Duin A C & Goddard III W A, *J Chem Theory and Computation*, 5 (2009) 1016.

36 Dennington R, Keith T & Millam J, GaussView, version 5. Semichem Inc.: Shawnee Mission, K S (2009).

37 Yanai T, Tew D P & Handy N C, *Chem Phys Lett*, 393 (2004) 51.

38 Chai J D & Head-Gordon M, *Phys Chem Chem Phys*, 10 (2008) 6615.

39 Cossi M, Barone V, Cammi R & Tomasi J, *Chem Phys Lett*, 255 (1996) 327.

40 Malashikhin S & Finney N S, *J Am Chem Soc*, 130 (2008) 12846.

41 van Heerden P S, Bezuidenhoudt B C & Ferreira D, *J Chem Soc Perkin Trans 1*, 1141 (1997).

42 Li W, Liu D, Shen F, Ma D, Wang Z, Feng T, Xu Y, Yang B & Ma Y, *Adv Funct Mater*, 22 (2012) 2797.

43 Tagare J, Ulla H, Satyanarayan M N & Vaidyanathan S, *J Luminescence*,194 (2018) 600.

44 Feng X, Xu Z, Hu Z, Qi C, Luo D, Zhao X, Mu Z, Redshaw C, Lam J W, Ma D & Tang B Z, *J Mater Chem*, *C*, 7 (2019) 2283.

45 Raj Gopal V, Mahipal Reddy A & Jayathirtha Rao V, *J Org Chem*, 60 (1995) 7966.

46 Mahipal Reddy A & Jayathirtha Rao V, *J Org Chem*, 57 (1992) 6727.

47 Goushi K, Yoshida K, Sato K & Adachi C, *Nat Photonics*, 6 (2012) 253.

48 Sasaki S, Drummen G P & Konishi G I, *J Mater Chem*, *C*, 4 (2016)2731.

49 Tanaka H, Shizu K, Nakanotani H & Adachi C, *Chem Mater*, 25 (2013) 3766.

50 Chidirala S, Ulla H, Valaboju A, Kiran M R, Mohanty M E, Satyanarayan M N, Umesh G, Bhanuprakash K & Jayathirtha Rao V, *J Org Chem*, 81 (2016) 603.

51 Nagaraju P, Madhu C, Mohanty M E & Jayathirtha Rao V, *Indian J Chem*, 57B (2018) 229.

52 Paulo J S, Gomes C S & Arnaut L G, *J Photochem Photobiol A*, 184 (2006) 228.

53 (a) Pommerehne J, Vestweber H, Guss W, Mahrt R F, Bässler H, Porsch M & Daub J, *Adv Mater*, 7 (1995) 551; (b) Bard A J, Faulkner L R, Leddy J & Zoski C G, *Wiley*, *New York*, 2 (1980).

54 Zhang G & Musgrave C B, *J Phys Chem*, *A*, 111 (2007) 1554.

55 Lakshmanan R, Sindhu & Nair S, *J Luminescence*, 168 (2010) 145.

56 Sasabe H & Kido J, *Chem Eur J*, 22 (2016) 1.